Ce–Sn intermetallic compounds as new anode materials for rechargeable lithium batteries

Hiroki Sakaguchi, Hitohiko Honda, Yuichi Akasaka, Takao Esaka[*]

Department of Materials Science, Faculty of Engineering, Tottori University, Minami 4-101, Koyama-cho, Tottori 680-8552, Japan

Abstract

To increase the volumetric discharge capacity of negative electrode for rechargeable lithium batteries, a new intermetallic compound including rare earth element, $CeSn_3$, was synthesized by mechanical alloying (MA), and the performance of the electrode was investigated. The $CeSn_3$ electrode was found to have a volumetric discharge capacity of over 2000 mA h cm^{-3} based on the theoretical volume of $CeSn_3$, which is three times larger than that of graphite electrode. The electrochemical reaction of the $CeSn_3$ electrode with Li may not obey the well-known mechanism of Li_xSn formation in the other tin-based electrodes because of lower potential plateaus in comparison with those of pure tin electrode. Although the $CeSn_3$ electrode exhibited very poor cycle life, performance could be improved significantly if the $CeSn_3$ was reacted with lithium using MA in advance. The resulting $Li_{3.8}CeSn_3$ electrode showed an excellent performance not only on the cyclability, but also on the reversibility at the first cycle.
© 2003 Elsevier Science B.V. All rights reserved.

Keywords: Lithium secondary battery; Anode material; $CeSn_3$; Lithium storage intermetallic compound

1. Introduction

Recently, intermetallic compounds as anode materials for rechargeable lithium batteries have been extensively investigated because of an increasing demand for higher capacity negative electrodes [1–19]. Among them, tin- [1–14] or silicon-based [15–17] intermetallic compounds appear to be promising anode materials for practical use, since they have large latent capacities in comparison with conventional carbon materials and exhibit better cyclability than binary alloys including lithium, such as Li_xAl and Li_xSn. However, large irreversible capacity at the first charge–discharge cycle and poor cyclability are still serious problems for practical use. These problems are caused by a considerable volume change in compound particle and/or grain refinement during deep cycling and the resulting disintegration.

Two approaches to stabilize the morphology of alloy electrodes have been suggested. One is the use of a multiphase alloy structure consisting of one active material phase and the other inactive phase served as a supporting and conducting matrix [1,3,5–8,13,15–17,19]. The nanostructured active phase is highly dispersed in the matrix phase, so that the disintegration of the compound particle is suppressed. Successful examples are Sn_xFe [1], Mg_2Si [17],

etc. Another effective approach is the use of an insertion of lithium into alloy lattice [2,9–11,14,18]. A few compounds, such as Cu_6Sn_5 [2] and Mg_2Ge [9–11,14], have been reported so far.

In this work, we focused on cerium in order to enhance the volumetric capacity of electrode because of its large density, and synthesized a new anode material, $CeSn_3$, using mechanical alloying (MA). The electrochemical performance of $CeSn_3$ electrode was investigated and the mechanism of electrode reaction was discussed. Furthermore, to solve the problems mentioned above, we attempted to prepare lithiated $CeSn_3$, i.e. $Li_{3.8}CeSn_3$, by mixing lithium with $CeSn_3$ using MA. The electrochemical characteristics of $Li_{3.8}CeSn_3$ were also examined as an alternative anode material.

2. Experimental

Experimental conditions of mechanical alloying to prepare $CeSn_3$ and $Li_{3.8}CeSn_3$ are as follows. Cerium chip (99.9%, ca. 1 mm, Santoku) and tin powder (99.99%, ca. 50 μm, Rare Metallic) were blended in a mole ratio of 1 (Ce):3 (Sn). The mixture was sealed in a stainless steel vessel (80 ml) together with five balls (φ 15) and milled using a high-energy planetary ball mill (Itoh, LP-4/2) in a dried argon atmosphere at 300 rpm. and at room temperature.

*Corresponding author. Tel.: +81-857-31-5264; fax: +81-857-31-5264.
E-mail address:* esaka@chem.tottori-u.ac.jp (T. Esaka).

The weight ratio of the balls to sample was about 15:1. In the same manner, $Li_{3.8}CeSn_3$ was synthesized with $CeSn_3$ powder (20 h MA, ca. 10 μm) and Li chip (99.98%, ca. 1 mm, Mitsui Mining & Smelting) as starting materials.

X-ray diffraction (Shimadzu, XRD-6000) was carried out using Ni-filtered Cu Kα radiation at a 2θ scan of $2°$ min^{-1} for phase identification of mechanically alloyed samples. A step-scanning method (2.4 s/$0.020°$) was applied to estimate lattice constants and the phases lithiated at different lithium-insertion steps. The chemical composition and impurities were determined with ICP emission spectroscope (Shimadzu, ICPS-5000). The particle size distribution was measured with Shimadzu SALD-2100 laser diffraction particle size analyzer giving an ultrasonic wave to reduce aggregate size. Furthermore, scanning electron micrographs of the sample powders were obtained to estimate a primary particle size.

Electrochemical performance of the electrodes was estimated with a three-electrode cell. The working electrode consisted of $CeSn_3$ or $Li_{3.8}CeSn_3$ powder (ca. 10 mg) and copper mesh (0.21 mm thick, 0.25 cm^2, 100 mesh). No conductive material and binder were used for the construction of the electrode. In the test cell, both counter and reference electrodes were 1 mm thick lithium metal sheets (99.98%) supplied by Mitsui Mining & Smelting. 1 M $LiClO_4$ dissolved in propylene carbonate from Kishida Reagents Chemicals was used as an electrolyte. The cell performance was estimated galvanostatically at a current density of 0.4 mA cm^{-2} for both charge and discharge at 303 K. Cyclic voltammetric measurements were carried out using the above mentioned three-electrode cell.

3. Results and discussion

Fig. 1 shows XRD patterns of the mechanically alloyed products using elemental Ce and Sn as starting materials. A single cubic phase appeared in the pattern after mechanical alloying for 20 h. A lattice parameter was calculated to be $a = 472.3$ pm which coincided with that of $CeSn_3$ (AuCu$_3$-type structure) which is available in the literature [20]. When the milling proceeded until 80 h, the diffraction peaks broadened slightly.

ICP analysis showed that the exact compositions are $CeSn_{3.1}Fe_{0.75}Cr_{0.38}Ni_{0.11}$, $CeSn_{3.5}Fe_{0.28}Cr_{0.03}Ni_{0.01}$, and $CeSn_{3.1}Fe_{0.83}Cr_{0.47}Ni_{0.08}$ for 20, 50, and 80 h MA samples, respectively. The impurities of Fe, Cr, and Ni must be derived from the mixing vessel and balls, because these are made of stainless steel. The concentration of impurities almost depends on the composition of the vessel. The 50 h MA sample exhibited a large fraction of tin in comparison with the other two samples. This may be due to that the removal of oxide from cerium as a starting material was insufficient only at the time, so that the amount of elemental cerium which contributes to an alloying reaction has decreased. As a result, an inside wall of vessel and balls
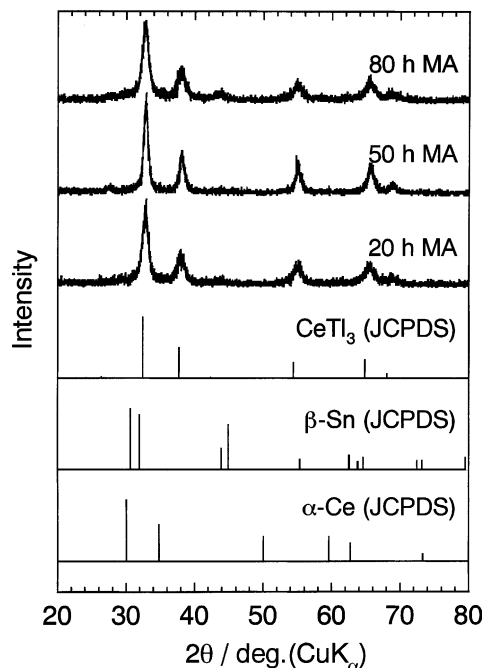

Fig. 1. Changes in XRD patterns of $CeSn_3$ with mechanical alloying (MA) time.

were covered with the excess tin, preventing the contamination from the vessel and balls. This appears to be a reason why the 50 h MA powders had much less impurity content than the others. Normally, this data should be deleted, but it will be left to discuss the influence of impurities on the electrode characteristics.

The particle sizes (aggregate size) for the 20, 50 and 80 h MA samples were estimated to be ca. 10, 1, and 1 μm, respectively. As shown in Fig. 2, SEM images of the sample powders are given to estimate a primary particle size. There was no so big difference of the primary particle size between 20 and 50 h MA samples.

Electrochemical measurements have been done for $CeSn_3$ electrodes prepared with a conductive material (graphite) and various binders. However, the best performance was obtained from the electrode without both conductive material or binder. Fig. 3 shows the charge–discharge (Li insertion–extraction) curves of $CeSn_3$ electrodes at the first cycle. The charge (Li insertion) capacity at the first cycle must include a surplus capacity owing to formation of solid electrolyte interface (SEI) layer and/or oxidation of lithium by oxygen dissolved in the alloy. In addition, the irreversible capacity at the first cycle may be caused by formation of electrically disconnected parts as a result of volume expansion due to lithium insertion and/or by excessive stabilization of lithium accommodated at defect sites in the alloy lattice. The charge–discharge capacities of both 20 and 80 h MA samples were a little bit smaller than that of the 50 h MA sample. This suggests that the impurities, such as Fe, Cr and/or Ni, obstruct the electrochemical reaction of $CeSn_3$ with lithium, because these elements hardly react with lithium. Mao et. al. reported that the precipitated Fe in SnFe makes
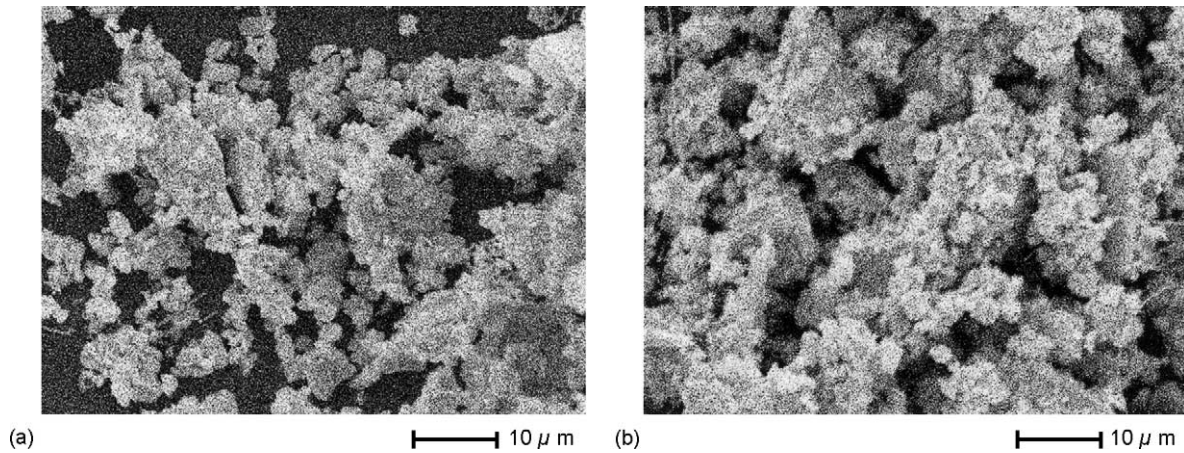
Fig. 2. SEM images of powders for (a) 20 h and (b) 50 h MA samples.

up a thin skin at the particle and/or grain surfaces and the skin prevents further Li reaction with the remaining alloy phase [1]. A similar phenomenon might occur in $CeSn_3$ containing high concentration impurities.

The gravimetric first discharge (Li extraction) capacities of the electrodes, ca. 280–350 mA h g^{-1}, were almost the same level as those of the graphite electrode. However, it was noteworthy that a volumetric discharge capacity of more than 2000 mA h cm^{-3}, which was translated using a density of $CeSn_3$, 7.83 g cm^{-3}, was much larger than that of the graphite electrode of ca. 800 mA h cm^{-3}. A density of the fully lithiated sample was calculated using a weighted average of Ce and $3Li_{4.4}Sn$ [21]. The resulting value was 3.82 g cm^{-3}. If one uses this density, the volumetric capacity was estimated to be about 1070 mA h cm^{-3} for the gravimetric capacity of 280 mA h g^{-1}.

If the reaction of $CeSn_3$ electrode with lithium proceeds according to the following displacement reaction: $CeSn_3 + 13.2Li \rightarrow Ce + 3Li_{4.4}Sn$, the theoretical capacity would be about 713 mA h g^{-1}. A large difference between the

experimental and theoretical values may suggest that the above displacement reaction had not proceeded completely. However, the morphology of the electrode varied obviously after lithium insertion and there has been no strong evidence to support the displacement reaction in this electrode. Therefore, we supposed that a different lithiation reaction unlike the displacement reaction occurs in the $CeSn_3$ electrode, as discussed below.

Considering a reaction mechanism of this electrode, we noted that potential plateaus in both charge and discharge curves were lower for $CeSn_3$ than for Sn alone. The $CeSn_3$ electrode exhibited potential plateaus at around 0.2 and 0.5 V, whereas the Sn electrode 0.4 and 0.6 V, respectively. The fact appears to indicate that the electrode reaction of $CeSn_3$ is not
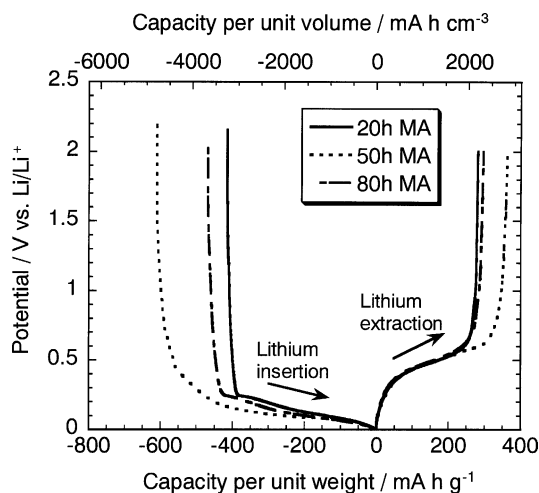

Fig. 3. The first charge–discharge curves for the electrodes of $CeSn_3$ synthesized at different MA time.
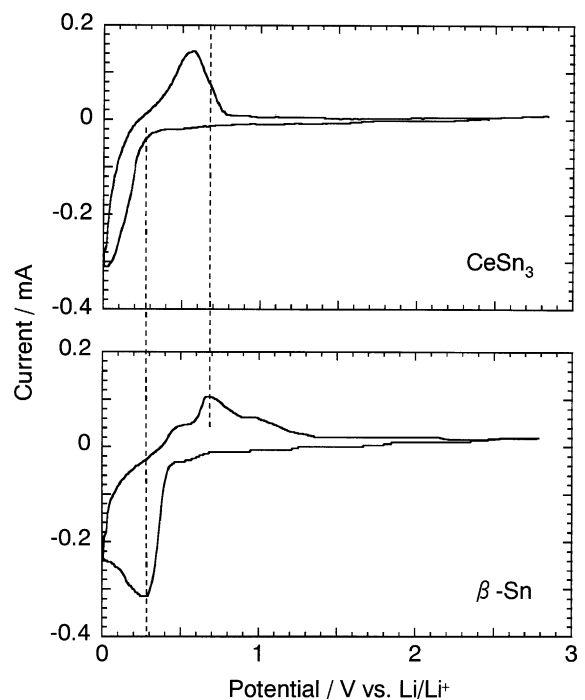

Fig. 4. Cyclic voltammograms (first cycle, 0.1 mV s^{-1}) for the $CeSn_3$ and Sn electrodes.

predominated by alloying–dealloying of $Li_{4.4}Sn$. To confirm whether $Li_{4.4}Sn$ forms or not, cyclic voltammetry was carried out on both $CeSn_3$ and Sn electrodes. As shown in Fig. 4, the cyclic voltammograms of $CeSn_3$ electrode were greatly different from those of Sn electrode, supporting the above idea. Furthermore, we should mention that the potential plateau remained at a lower potential than the elemental tin electrode for the second and subsequent cycles. The lowering of potential plateau could be due to the difference of electronic state between tin in $CeSn_3$ and elemental tin. If the displacement reaction, i.e. formation of $Li_{4.4}Sn$, is predominant, the potential plateau should appear at the almost same position as elemental tin, as reported for Fe–Sn alloys [1]. Therefore, this may support that $CeSn_3$ does not decompose even after electrochemical lithiation.

Fig. 5 shows XRD patterns of $CeSn_3$ obtained at different lithium-insertion steps. The XRD experiments were carried out ex situ using the samples separately prepared at each potential. No new phase, such as Li_xSn or β-Sn, appeared and no peak shift toward lower angle side was observed at any indicated potentials and even after 20 cycles, though the peak intensity decreased gradually. This result would deny the formation of Li–Sn alloys and an interstitial solid solution, Li_xCeSn_3, i.e. lithium insertion into the interstitial of $CeSn_3$ lattice. There is a possibility of formation of a substitutional solid solution, i.e. tin atoms in $CeSn_3$ are substituted by lithium atoms, because slight peak shifts
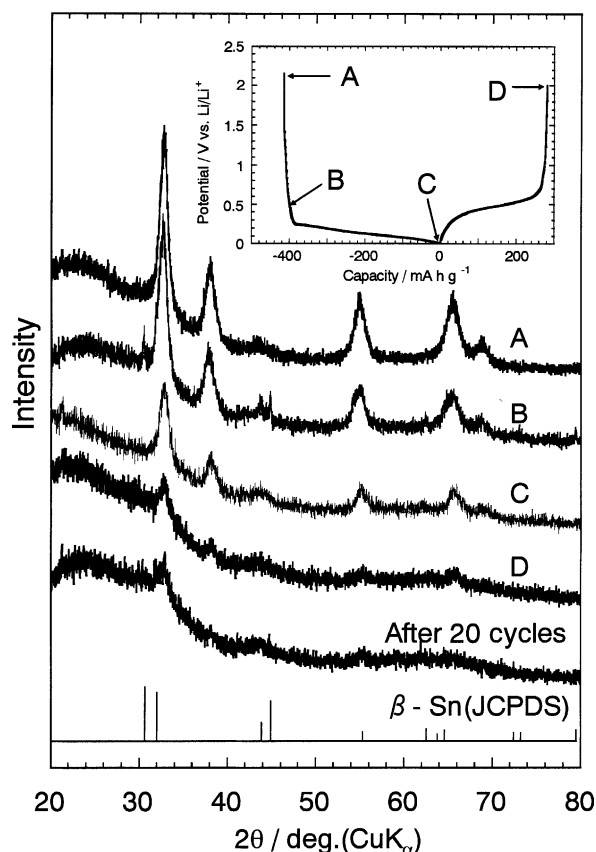
toward higher angle side were observed in the fully lithiated sample (step C). The precipitated tin would be finely dispersed, so that it could not be detected by X-ray diffraction. Although being coated with a silicone grease and dimethyl-naphthalene to avoid oxidation, the sample powders oxidize occasionally. We have observed in another XRD experiment that an elemental tin phase appears after exposing $CeSn_3$ into the air, and the tin phase grows with the exposed time, indicating that the precipitation of tin occurred by oxidation of cerium in $CeSn_3$. Therefore, we believe that the elemental tin observed at the potential C was caused not by the electrochemical reaction, but by the oxidation of the sample during the XRD measurement.

As mentioned above, there has been no clear evidence to support the displacement reaction in this electrode. Furthermore, the morphology of electrode varied obviously after lithium insertion and no new phase appeared in the electrochemically lithiated sample. Consequently, we supposed that a different lithiation reaction unlike the displacement reaction occurs in the $CeSn_3$ electrode, and proposed a reaction of formation of a substitutional solid solution, as one of the possibilities. To prove this reaction, the neutron elastic scattering experiment on the electrochemically lithiated sample is under investigation.

Fig. 6 displays cyclability of discharge capacity for the electrodes of $CeSn_3$ synthesized by different MA time. Unfortunately, the $CeSn_3$ electrode exhibited poor performance for cycle life. In our previous study for the Mg_2Ge electrode, it has been suggested that the charge–discharge capacity is strongly affected by milling time, i.e. change in structure and/or internal energy generated by mechanical milling, and the appropriate increase in internal energy is necessary to maintain the capacity during the repeated cycling [10,11]. For the $CeSn_3$ electrode, however, there was very little difference of electrode performance between the 20 and 80 h MA samples. The prolonging in MA time may not influence the structure and/or internal stress of $CeSn_3$.

Since there are some reports that the capacity retention characteristics for the other tin-alloy electrodes were

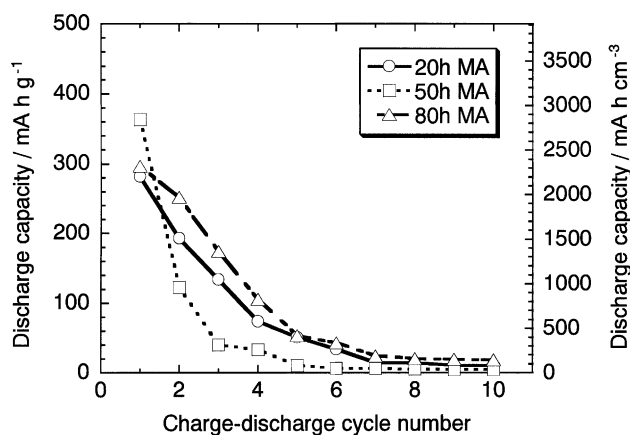Fig. 5. XRD patterns of $CeSn_3$ at various lithiated steps.

Fig. 6. Cyclability of discharge capacity for the electrodes of $CeSn_3$ synthesized at different MA time.
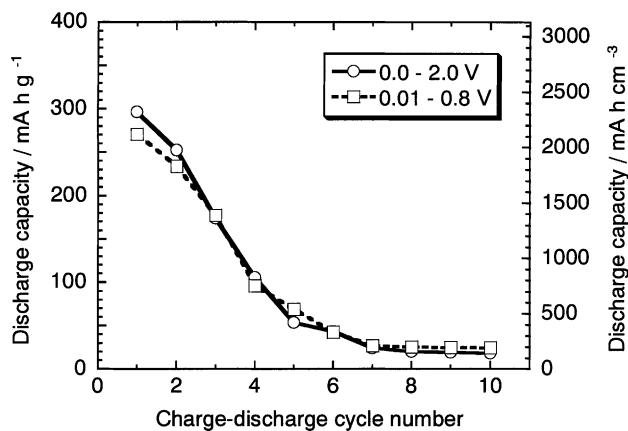
Fig. 7. Cyclability of discharge capacity for the CeSn$_3$ (20 h MA) electrode under restricted voltage region.

Fig. 9. Cyclability of discharge capacity for the Li$_{3.8}$CeSn$_3$ and CeSn$_3$ electrodes.

improved by controlling voltage range [1,2,13], this was attempted with the CeSn$_3$ electrode. Fig. 7 illustrates the cycle life performance of CeSn$_3$ electrode under two operating voltage ranges. The cyclability could not be improved when the upper and lower cut-off voltages were restricted to 0.8 and 0.01 V versus Li/Li$^+$. The behavior was quite different from that of the other tin-based intermetallic compounds that the electrode reaction proceeds according to Li–Sn alloy formation.

The poor cycle life performance of CeSn$_3$ electrode appears to be due to grain refinement during cycle and subsequent a lack of electrical conductivity. To prevent the grain refinement, we tried to add lithium as a third element into CeSn$_3$. To put it concretely, CeSn$_3$ (20 h MA sample) and elemental lithium were blended and the mixture was mechanically alloyed for 20 h. Charge–discharge curves and cycle life performance of the resulting Li$_{3.8}$CeSn$_3$ electrode are shown in Figs. 8 and 9, respectively. The Li molar ratio of 3.8 corresponds to a half of the charge capacity for the 20 h MA CeSn$_3$ electrode (Fig. 5). Surprisingly, a discharge coefficient of Li$_{3.8}$CeSn$_3$ electrode was estimated to be more than
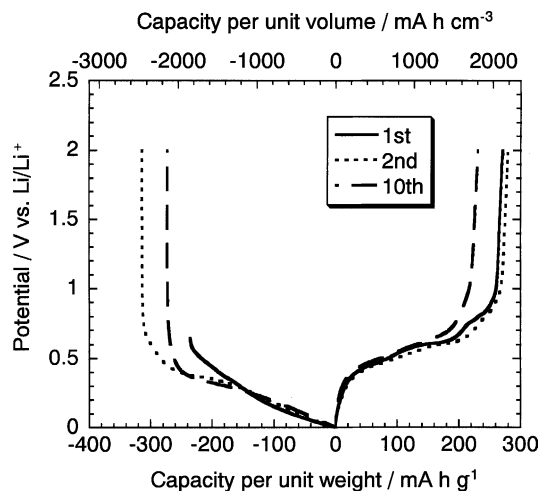
100% at the first cycle, suggesting that a part of lithium involved in Li$_{3.8}$CeSn$_3$ was also spent to the discharge reaction. Moreover, the cyclability was found to be remarkably improved on the electrode. Mane studies of the Li$_{3.8}$CeSn$_3$ are presently underway.

4. Conclusions

CeSn$_3$ synthesized by mechanical alloying was found to electrochemically absorb and desorb lithium without any conductive materials and binders. The volumetric discharge (lithium extraction) capacity of the CeSn$_3$ electrode was estimated to be more than 2000 mA h cm^{-3} which is three times larger than that of graphite electrode, but to be ca. 1070 mA h cm^{-3} if one used a density of the fully lithiated sample which is derived from a weighted average of Ce and 3Li$_{4.4}$Sn. A reaction mechanism of CeSn$_3$ electrode may be different from that of the other tin-based alloy electrodes, since evidences of Li$_x$Sn formation could not be obtained. Poor cycle life performance of CeSn$_3$ electrode was drastically improved by mechanically adding lithium to CeSn$_3$. Furthermore, the Li$_{3.8}$CeSn$_3$ electrode exhibited no irreversible capacity at the first charge–discharge cycle.

Fig. 8. Charge–discharge curves of the Li$_{3.8}$CeSn$_3$ electrode.

References

[1] O. Mao, J.R. Dahn, J. Electrochem. Soc. 146 (1999) 414.
[2] K.D. Kepler, J.T. Vaughey, M.M. Thackeray, Electrochem. Solid-State Lett. 2 (1999) 307.

[3] D. Larcher, L.Y. Beaulieu, D.D. MacNeil, J.R. Dahn, J. Electrochem. Soc. 147 (2000) 1658.

[4] D.G. Kim, H. Kim, H.-J. Sohn, T. Kang, J. Power Sources 104 (2002) 221.

[5] J. Yang, M. Winter, J.O. Besenhard, Solid State Ion. 90 (1996) 281.

[6] J.O. Besenhard, M. Wachtler, M. Winter, R. Andreaus, I. Rom, W. Sitte, J. Power Sources 81/82 (1999) 268.

[7] J. Yang, Y. Takeda, N. Imanishi, O. Yamamoto, J. Electrochem. Soc. 146 (1999) 4009.

[8] G.M. Ehrlich, C. Durand, X. Chen, T.A. Hugener, F. Spiess, S.L. Suib, J. Electrochem. Soc. 147 (2000) 886.

[9] H. Sakaguchi, H. Honda, T. Esaka, Denki Kagaku 66 (1998) 1291.

[10] H. Sakaguchi, H. Honda, T. Esaka, J. Power Sources 81/82 (1999) 229.

[11] H. Sakaguchi, H. Honda, H. Maeta, T. Esaka, The Japan Institute of Metals Proceedings (JIMIC-3) 12 (1999) 1305.

[12] H. Sakaguchi, H. Maeta, H. Honda, T. Esaka, Electrochemistry 68 (2000) 632.

[13] H. Kim, Y.-J. Kim, D.G. Kim, H.-J. Sohn, T. Kang, Solid State Ion. 144 (2001) 41.

[14] H. Honda, H. Sakaguchi, T. Fukunaga, T. Esaka, Electrochemistry 70 (2002) 99.

[15] A. Anani, R.A. Huggins, J. Power Sources 38 (1992) 351.

[16] W.J. Weydanz, M. Wohlfahrt-Mehrens, R.A. Huggins, J. Power Sources 81/82 (1999) 237.

[17] H. Kim, J. Choi, H.-J. Sohn, T. Kang, J. Electrochem. Soc. 146 (1999) 4401.

[18] J.T. Vaughey, J.O. O'Hara, M.M. Thackeray, Electrochem. Solid-State Lett. 3 (2000) 13.

[19] K.C. Hewitt, L.Y. Beaulieu, J.R. Dahn, J. Electrochem. Soc. 148 (2001) A402.

[20] F. Ruggier, Accand. Naze. Lincei Rend. Classe Sc. Fis. 37 (1964) 169.

[21] M. Winter, J.O. Besenhard, Electrochim. Acta 45 (1999) 31.